# Kinetics of GPIb$\alpha$-vWF-A1 Tether Bond under Flow: Effect of GPIb$\alpha$ Mutations on the Association and Dissociation Rates

R. Anand Kumar,* Jing-fei Dong,† Jenny A. Thaggard,† Miguel A. Cruz,† José A. López,† and Larry V. McIntire*

*Department of Bioengineering, Rice University, Houston, Texas; and †Thrombosis Research Section, Department of Medicine, Baylor College of Medicine, Houston, Texas

ABSTRACT The interaction between platelet glycoprotein (GP) Ib-IX-V complex and von Willebrand factor (vWF) is the first step of the hemostatic response to vessel injury. In platelet-type von Willebrand disease, two mutations, G233V and M239V, have been described within the $Cys^{209}$-$Cys^{248}$ disulfide loop of GPIb$\alpha$ that compromise hemostasis by increasing the affinity for vWF. We have earlier shown that converting other residues in this region to valine alters the affinity of GPIb$\alpha$ for vWF, with mutations K237V and Q232V, respectively, showing the greatest increase and decrease in affinity. Here, we investigated further the effect of these two mutations on the kinetics of the GPIb$\alpha$ interaction with the vWF-A1 domain under dynamic flow conditions. We measured the cellular on- and off-rate constants of Chinese hamster ovary cells expressing GPIb-IX complexes containing wild-type or mutant GPIb$\alpha$ interacting with vWF-A1-coated surfaces at different shear stresses. We found that the gain-of-function mutant, K237V, rolled very slowly and continuously on vWF-A1 surface while the loss-of-function mutant, Q232V, showed fast, saltatory movement compared to the wild-type (WT). The off-rate constants, calculated based on the analysis of lifetimes of transient tethers formed on surfaces coated with limiting densities of vWF-A1, revealed that the Q232V and K237V dissociated 1.25-fold faster and 2.2-fold slower than the WT. The cellular on-rate constant of WT, measured in terms of tethering frequency, was threefold more and threefold less than Q232V and K237V, respectively. Thus, the gain- and loss-of-function mutations in GPIb$\alpha$ affect both the association and dissociation kinetics of the GPIb$\alpha$-vWF-A1 bond. These findings are in contrast to the functionally similar selectin bonds where some of the mutations have been reported to affect only the dissociation rate.

## INTRODUCTION

In response to a vascular injury, platelets adhere to the subendothelial matrix, which sets off a sequence of signal events in the platelet that result in activation, spreading on the exposed matrix, granule release, and aggregation to form a hemostatic plug. The entire process is initiated by an interaction between the glycoprotein (GP) Ib-IX-V complex on the platelet surface and immobilized von Willebrand factor (vWF) on the exposed subendothelium (Andrews et al., 1997).

Soluble vWF circulates in blood plasma and immobilized vWF is found in the subendothelial matrix. vWF is a multimer made up of several monomers and each monomer is composed of 11 functional domains—D1, D2, D′, D3, A1, A2, A3, D4, B, C1, and C2 in the order spanning from N- to C- terminus (Sadler, 1998). The A1 domain of vWF, which spans amino acids $Cys^{509}$–$Cys^{695}$, has been identified as containing the binding site for the GPIb-IX-V complex (Miyata and Ruggeri, 1999).

The GPIb-IX-V complex contains four transmembrane polypeptide chains, GPIb$\alpha$, GPIb$\beta$, GPIX, and GPV (López and Dong, 1997). The complex associates with the platelet cytoskeleton and signal transduction proteins through which activation signals are processed. The ligand-binding site of vWF has been mapped to the GPIb$\alpha$ subunit (Berndt et al., 2001). The GPIb$\alpha$ subunit has three major structural features in its extracellular domain: a leucine-rich repeat motif, with conserved N- and C-terminal flanking disulfide loops (residues 1–268), an extremely anionic region containing three sulfated tyrosines and the binding site for thrombin (269–287), and a highly O-glycosylated region between the leucine-rich repeat region and the transmembrane region that serves as a spacer (Fig. 1) (López, 1994). The binding site for vWF is contained in the 45-kDa N-terminal region of ~300 amino acids. Mutations that increase the affinity of GPIb$\alpha$ for vWF have been localized to the first of two C-terminal disulfide loops in the leucine-rich repeat region (see Fig. 1). These mutations produce a disease called platelet type von Willebrand disease (ptVWD) which is paradoxically associated with mild to moderate bleeding because the abnormally reactive receptor binds and clears the most hemostatically active large multimers of vWF from the circulation (Miller, 1996). Two cases of ptVWD result from a substitution of Val for Gly at residue 233 (G233V) and Val for Met at residue 239 (M239V). Both mutations are close to each other in the primary structure of the polypeptide within the $Cys^{209}$-$Cys^{248}$ disulfide loop (Fig. 1). It has recently been shown from the cocrystal structure of GPIb$\alpha$ with vWF-A1 that this region is directly involved in the binding to vWF (Huizinga et al., 2002).

It is of interest to note that, not only do these mutations affect the residues in close proximity to each other in the linear sequence of GPIb$\alpha$, but both mutations also convert existing nonvaline aminoacids to valine. We have previously exam-

*Submitted April 4, 2003, and accepted for publication August 12, 2003.*

Address reprint requests to Larry V. McIntire, PhD, Department of Biomedical Engineering, Georgia Tech and Emory University, 313 Ferst Drive, Suite 2116, Atlanta, Georgia 30332-0535. Tel.: 404-894-5057; Fax: 404-385-5028; E-mail: larry.mcintire@bme.gatech.edu.



0006-3495/03/12/4099/11 $2.00

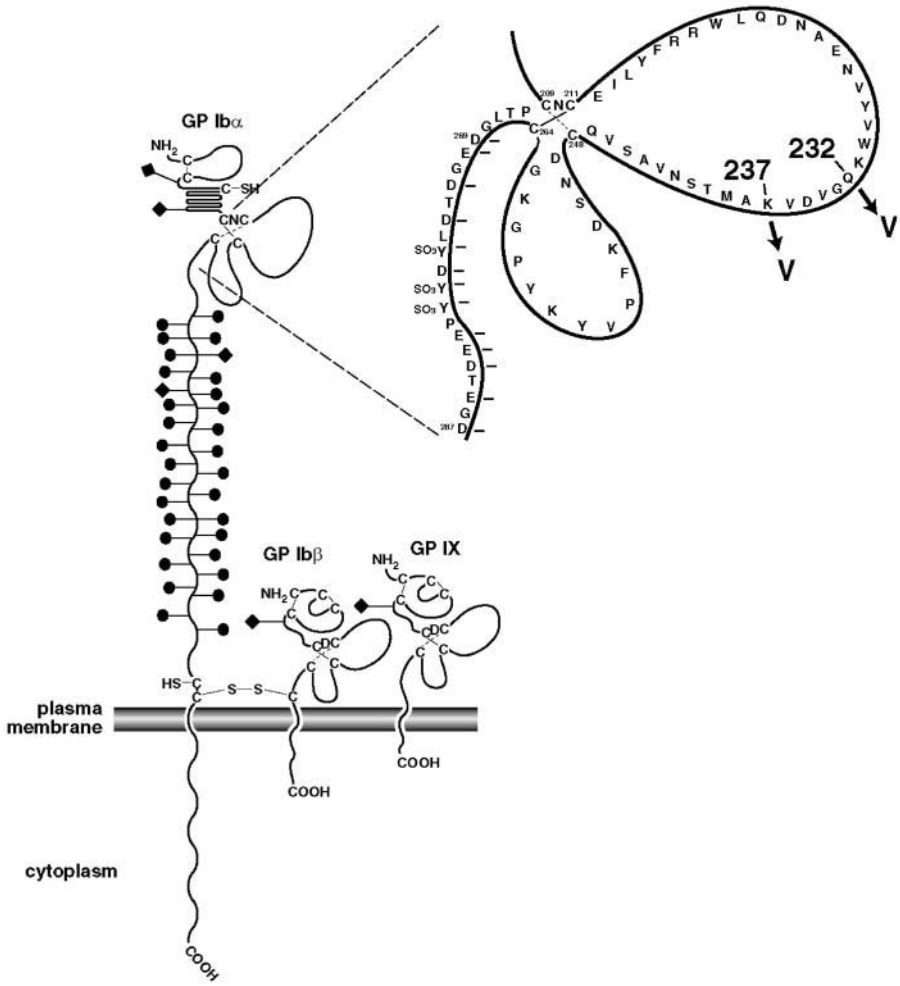


FIGURE 1 The GPIb-IX complex. The drawing depicts the structural domains of the three subunits of the GPIb-IX complex along with an exploded view of the disulfide loop region of GPIbα. The mutations used in this study, K237V and Q232V, are highlighted. Solid circles and diamonds attached to the stalks represent O-linked and N-linked carbohydrates respectively.

ined the effect of converting other nonvaline residues in this region to valine on the function of GPIb-IX-V complex under static and dynamic conditions (Dong et al., 2000, 2001). Two mutations—D235V and K237V—in addition to the naturally occurring G233V and M239V, displayed a gain-of-function phenotype. In contrast, some of the other valine mutations in this region resulted in a loss-of-function phenotype including N226V, K231V, Q232V, and A238V. The gain-of-function mutants bound vWF spontaneously and had a heightened response to low concentrations of ristocetin or botrocetin, whereas the loss-of-function mutants bound vWF poorly compared to the wild-type GPIbα. Also, on immobilized vWF, the gain-of-function mutants showed a decrease and the loss-of-function mutants showed an increase in the rolling velocities respectively, suggesting that these mutations affected the binding kinetics of GPIbα-vWF interaction. Among the gain-of-function mutants, K237V rolled the slowest, and among the loss-of-function mutants, Q232V rolled the fastest compared to the wild-type (WT). For instance, at 5 dyn/cm$^2$, the rolling velocities of Q232V (140 $\mu$m/s) and of K237 (20 $\mu$m/s) were, respectively, 2.5-fold more and threefold less than that of wild-type (60 $\mu$m/s) (Dong et al., 2000). We had speculated that the difference in rolling velocities could primarily be due to the differences in the dissociation binding kinetics of bonds that mediate the rolling process.

Recently, a few investigators have studied the kinetics of interaction of wild-type and gain-of-function mutants of GPIbα with vWF (Miura et al., 2000; Huizinga et al., 2002; Doggett et al., 2002, 2003). Miura et al. (2000) attributed the difference in affinities for mutant and wild-type GPIbα to the difference in the association rates of vWF and GPIbα. Using a static biochemical assay, for wild-type GPIbα-vWF-A1 interaction, they measured the association rate constant ($k_{on}$) to be 1100 M$^{-1}$ s$^{-1}$ and the dissociation rate constant ($k_{off}$) to be 0.0038 s$^{-1}$. They also reported that the increase in affinity caused by type2B (mutation I546V in vWF-A1 domain that increases the affinity of vWF-A1 for GPIbα) and ptVWD mutations is due to a fourfold increase in the $k_{on}$ even though the $k_{off}$ remains unchanged compared to the wild-type. In contrast to these studies, Doggett et al. (2002) reported a 1000-fold higher dissociation rate constant for wild-type GPIbα-vWF-A1 interaction than that reported by Miura et al. (2000) and also showed that the increase in affinity in type2B

VWD is due to a fivefold decrease in the dissociation rate. Using surface plasmon resonance, Huizinga et al. (2002) reported a dissociation equilibrium constant ($K_D$) of the GPIbα-vWF-A1 interaction of 30 nM. This value is 100-fold lower than that reported by Miura et al. (2000). Very recently, Doggett et al. (2003) reported that alteration in the kinetics of GPIbα-vWF-A1 interaction because of the ptVWD mutation is due to both enhanced cellular on-rate and decreased off-rate. Thus, considerable controversy exists in the measurement of the kinetic constants of this biologically important interaction and also as to whether the increase in affinity in type2B or ptVWD mutations is due to alterations in association or dissociation rate.

In this article, we have studied the kinetics of GPIbα-vWF-A1 interactions and quantified the association and dissociation rate constants for both wild-type and mutant GPIbα interaction with vWF-A1. We have used Chinese hamster ovary (CHO) cells expressing wild-type and mutant GPIbα interacting with immobilized vWF-A1 as our model system. To study the effect of mutations on the kinetics of this interaction, we used cells expressing GPIbα carrying mutations K237V and Q232V as representatives of the gain- and loss-of-function phenotypes, because these two mutants showed the strongest and weakest interactions in both static and dynamic adhesion assays (Dong et al., 2000). These two mutations are located in the disulfide loop formed by a bond between $Cys^{209}$ and $Cys^{248}$ (Fig. 1). We used tethering frequency—the rate at which cells are captured to the vWF-A1 surface from free flow—as a measure of effective or cellular $k_{on}$ and the lifetime of transiently tethered cells to measure $k_{off}$. We demonstrate that the tethering frequency ($k_{on}$) for the WT is threefold lower and threefold higher than those of K237V and Q232V, respectively, while the estimated unstressed dissociation rate constant ($k^0_{off}$) of the WT is 1.25-fold lower and 2.2-fold higher than those of Q232V and K237V, respectively. Our results suggest that both the association and dissociation rates are important in contributing to the phenotypic differences. The kinetic analysis of the implications of gain-of-function mutation (K237V) will help us to better understand the functionally similar, naturally occurring ptVWD mutations and also might aid in the development of therapeutics based on a quantitative analysis. This is the first time that the kinetic effects of a loss-of-function mutation (Q232V) of GPIb has ever been studied and our results could be important in understanding the fundamental mechanisms of cell rolling and adhesion.

## MATERIALS AND METHODS

### Cell lines

Chinese hamster ovary cells were transfected with either wild-type or mutant DNA for GPIbα, wild-type DNA for GPIbβ, and GP IX as described elsewhere (López et al., 1994). The cell lines used in this study and the receptor expression are given in Table 1. The cells were grown in α-MEM medium (Life Technologies, Grand Island, NY) supplemented with 10% fetal bovine serum. Selection drugs used for CHO βIX cells were 400 μg/ml G418 (Life Technologies) and 80 μM methotrexate (Sigma Chemical, St. Louis, MO). For the wild-type and mutant cells, along with these two selection drugs, 400 μg/ml Hygromycin B (Sigma Chemical) was used. All cells were maintained at 37°C with 5% $CO_2$.

**TABLE 1 Cell lines used in this study**

| Cell line | Abbreviation | Expression |
|---|---|---|
| CHO βIX | B9 | GPIbβ, GP IX (Control) |
| CHO αβIX | WT | GPIbα, GPIbβ, GP IX |
| CHO βIX/α232 | Q232V | GPIbβ, GP IX, GPIb α232 mutant (Glu-232 to Val) |
| CHO βIX/α233 | K237V | GPIbβ, GP IX, GPIb α237 mutant (Lys-237 to Val) |

### Flow cytometry

Flow cytometry was used to determine the cell surface expression levels of the wild-type and mutant GPIb-IX complex. CHO cells expressing the wild-type or mutant polypeptides were detached with 0.53 mM EDTA, washed with phosphate-buffered saline (PBS), and incubated with FITC-conjugated mouse monoclonal (AK2 clone) antibody to CD42b receptor (Research Diagnostics, Flanders, NJ) for 60 min at room temperature. This antibody binds subunits 1–59 of GPIbα (Shen et al., 2000). The cells were then analyzed on a FACScan flow cytometer (Becton Dickinson, San Jose, CA), stimulating with 488-nm laser light and collecting light emitted at >530 nm. Nonspecific binding was determined by the background fluorescence from CHO βIX cells stained with the same antibody. The data were analyzed using Cellquest software from Becton Dickinson. The cells were repeatedly sorted for GPIb-IX expression with antibody-coupled magnetic beads to maintain comparable expression levels between the wild-type and mutant GPIbα cells. The GPIbα surface density was estimated by measuring the number of binding sites available for FITC-conjugated AK2 antibody. The number of binding sites was determined by comparing the fluorescent intensity of the sample against that of a set of calibrated beads carrying a known number of antibody binding sites (Flow Cytometry Standards, San Juan, Puerto Rico).

### Preparation of vWF-A1 coated coverslips

The recombinant vWF-A1 was produced in *Escherichia coli* and purified as described previously (Cruz et al., 2000). Glass coverslips (No. 1, 24 × 50 mm, Corning, Corning, NY) were coated with a 5-mm diameter, 20-μL spot of vWF-A1 solution (diluted to appropriate concentrations with PBS) and incubated for 60 min at room temperature in a humid chamber. The coverslips were then rinsed with 1 ml of PBS and coated with 200 μl of 5% human serum albumin (HSA) solution for 60 min at room temperature to block any nonspecific binding. Any excess HSA was rinsed off with 1 ml of 0.9% saline before assembly as the bottom of a parallel-plate flow chamber. The binding of vWF-A1 to glass coverslips was determined by an enzyme linked immunosorbent assay (ELISA) using horseradish peroxidase (HRP)-conjugated anti-6-His monoclonal antibody (Sigma) that binds to the 6-His tag of the recombinant vWF-A1. The amount of vWF-A1 adsorbed on the surface at different vWF-A1 coating solution concentrations was measured in terms of absorbance of *o*-phenylenediamine/$H_2O_2$ solution at 490 nm ($A_{490}$). The number of binding sites was read from a calibration standard correlating the measured $A_{490}$ values at different known quantities of anti-6-His antibody in solution.

### Parallel plate flow chamber and digital image processing

Cells were perfused through the parallel plate flow chamber placed on an inverted-stage phase-contrast microscope (DIAPHOT-TMD; X-20 or X-10

phase objective and X-5 projection lens, Nikon, Garden City, NY). The parallel-plate flow chamber consisted of a polycarbonate slab, a silicone gasket creating a defined gap, and a glass coverslip coated with vWF-A1 held together by application of a vacuum (Slack and Turitto, 1994). The chamber was maintained at 37°C by an air curtain incubator attached to the microscope. The wall shear stress depends on the height of the gap, the width of the chamber, the fluid viscosity and the flow rate through the chamber (Ross et al., 1998). Cells resuspended to the desired concentration were perfused through syringe pump (Harvard Apparatus, Hollison, MA) and the microscopic images of cells were videotaped at 30 fps using a silicon-intensified target video camera (Model C2400; Hammatsu, Waltman, MA) attached to the microscope. The digitized images were collected off-line and analyzed using ISee software (InoVision, Durham, NC).

### Measurement of rolling velocities

Velocities of rolling cells were measured by tracking the displacements of individual cells frame by frame, every 0.033 s, in the direction of flow (Nanotrack, Inovision). For each experiment, at least 50 cells were tracked up to a maximum time period of 10 s. To differentiate cells rolling on the surface from the cells in free flow, we used a velocity threshold cut-off, below which the cells are believed to be in contact with the surface. The velocity threshold was determined based on the velocity at which tethered cells are released from the surface back into the fluid stream. At 1.6 dyn/cm$^2$, the distribution of release velocities was approximately normally distributed ($n = 150$) with a mean of 260 $\mu$m/s and a SD of 60 $\mu$m/s. Hence, >97% of the cells traveling at a velocity <80 $\mu$m/s are likely to be in contact with the surface. Hence, 80 $\mu$m/s was chosen as the operational threshold to separate cells in contact with the surface from cells free in flow. Only cells that stayed in contact with the surface for at least 0.2 s were considered for rolling. The time spent by a cell during one continuous sequence of velocities below the velocity threshold is defined as the rolling duration and rolling velocity was calculated from the distance moved in this period.

### Tethering rate and adhesion strength

CHO cells expressing GPIb-IX complex were perfused into the flow chamber at a concentration of $10^6$ cells/ml over vWF-A1 coated coverslips. The cell concentration at the inlet was maintained at similar levels and the fields of view were chosen at approximately the same distance from the inlet to minimize any effect of variations in the cell flux with distance from the inlet. The rate at which the free-flowing cells tethered to the surface was measured during the first 60 s of perfusion. The tethering rate at different shear stresses was normalized by dividing the number of cells tethered by the number of cells transported across the field of view in the focal plane of the immobilized vWF-A1. The tethering rates for WT, Q232V, and K237V cells were corrected for any nonspecific interaction by subtracting out the background values obtained for CHO $\beta$IX cells (lacking GPIb$\alpha$) under identical conditions. To measure the strength of adhesion, detachment assays were performed as follows: cells were allowed to accumulate at low shear stress (0.5 dyn/cm$^2$) for 3 min. Any nonadherent cells were washed off by perfusing cell-free buffer and the wall shear stress was doubled every 30 s and the number of cells remaining adherent on the surface was counted.

### Pause-time analysis

The interaction lifetime between CHO cells expressing the GPIb-IX complex and vWF-A1 adsorbed surfaces was quantified by analyzing the transient tethering events. A transient tethering event is defined as the abrupt stoppage of a free-flowing cell without evidence of its translocation on the surface before rejoining the bulk flow, to resume a velocity equivalent to that of a noninteracting cell. We used vWF-A1 concentrations lower than would support continuous rolling of CHO cells (15–55 $\mu$g/ml). This ensures that the cell does not roll and is probably tethered to the surface by the basic binding unit that mediates the interaction under such conditions (Alon et al., 1997; Ramachandran et al., 1999). We recorded ~150–250 such events at each shear stress for each of the mutants at a spatial resolution of 1 $\mu$m and a temporal resolution of 1/30 s. We used first-order dissociation kinetics, $dN_b/dt = -k_{off} N_b$, to fit the tether duration distribution, where $N_b$ is the number of bound cells. The resultant plot is a straight line with slope = $-k_{off}$, the dissociation rate constant. At least three independent measurements of $k_{off}$ were made with both the mutants and wild-type at each wall shear stress examined.

## RESULTS

### Interaction of GPIb-IX cells with vWF-A1-coated surfaces

The level of surface expression of GPIb$\alpha$ in cells expressing wild-type GPIb$\alpha$ or the mutants K237V and Q232V along with CHO $\beta$IX control is shown in Fig. 2 *A*. It can be seen from the fluorescence plots for the cell samples that the GPIb$\alpha$ expression in the mutants and wild-type are equivalent. We maintained the expression at such comparable levels so that the functional differences observed in our experiments are intrinsic and not due to differences in the receptor densities. The GPIb$\alpha$ receptor density was estimated as the number of AK2 binding sites to be ~100/$\mu$m$^2$. CHO cells expressing GPIb$\alpha\beta$-IX complex were perfused over immobilized vWF-A1 coated surfaces at different shear stresses. The interaction of the cells with the surface was specific for GPIb$\alpha$-vWF-A1 interaction because neither did the CHO cells expressing GPIb$\alpha\beta$-IX (WT, K237, and Q232V) interact with HSA coated surfaces nor did cells expressing only GPIb$\beta$-IX (without GPIb$\alpha$) interact with vWF-A1 coated surfaces. The adsorption of vWF-A1 as a function of vWF-A1 coating solution concentration was calculated in terms of absorbance at 490 nm (Fig. 2 *B*). The vWF-A1 site densities were estimated to be 72, 228, 351, and 415 sites/$\mu$m$^2$ for vWF-A1 coating solution concentrations of 10, 30, 70, and 100 $\mu$g/ml, respectively.

### Detachment strength

We performed a detachment assay by perfusing the WT or mutant cells on vWF-A1 surface at low shear stress and then increasing the shear stress progressively to detach adherent cells. We found that even at 0.5 dyn/cm$^2$, Q232V formed only brief tethers with the surface while WT rolled for very short distances before detaching spontaneously. The K237V cells rolled on the surface and detached slowly when the shear stress was increased (Fig. 3). Only ~50% of the cells detached even at a shear stress of 16 dyn/cm$^2$, indicating that the K237V-vWF-A1 interaction has either a very low dissociation rate (very long lifetime) or a high association rate that results in the formation of many new bonds as the cell moves, thus strengthening the interaction.

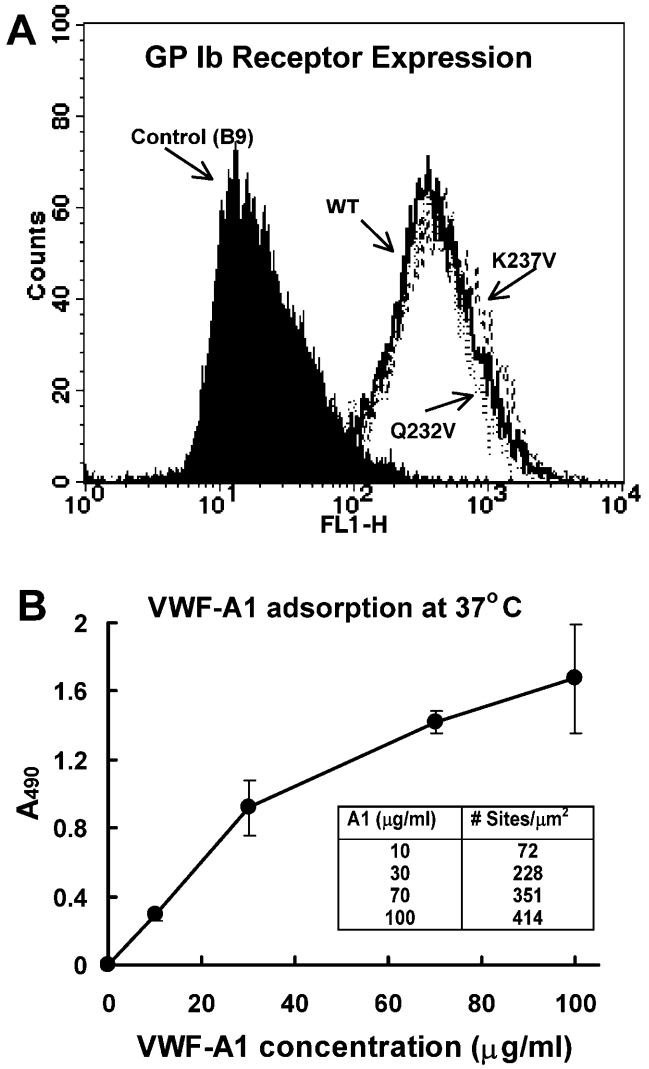


FIGURE 2 (*A*) Cell surface expression of GPIbα (WT, Q232V, and K237V) on transfected CHO cells: The cells were incubated with FITC-conjugated mouse monoclonal antibody AK2 in 5% HSA solution for 60 min. The expression levels were detected using FACScan flow cytometry. CHO cells expressing GPIbβ-IX (without α-subunit) were used as control. (*B*) Adsorption of VWF-A1 on glass coverslips at 37°C. The absorbance values are averaged from two experiments performed in triplicate.

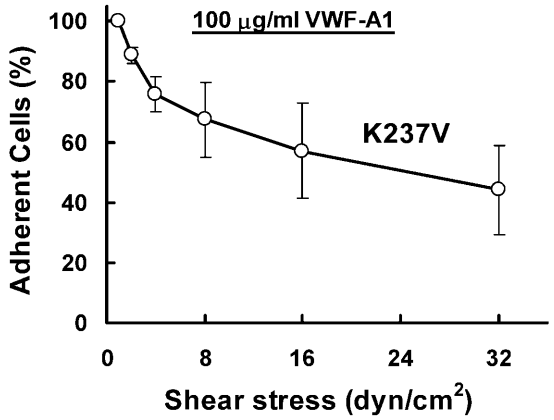


FIGURE 3 Detachment strength of GPIbα-VWF-A1 tethers: Cells expressing WT and mutant GPIbα were allowed to accumulate at 0.5 dyn/cm$^2$ shear stress on surfaces coated with 100 μg/ml VWF-A1 solution for 3 min. Then cell-free buffer was perfused and the shear stress was doubled every 30 s. The percentage of cells remaining adherent was determined. The data represent mean ± SD of three experiments. Q232V and WT did not form stable tethers even at low shear stresses: although most of the Q232V cells moved a fraction of the cell diameter before detachment, the majority of the WT cells moved a few cell diameters before spontaneously rejoining the flow.

## Kinetics of rolling of CHO cells expressing wild-type and mutant GPIbα on vWF-A1 coated surfaces

We studied the kinetics of rolling based on instantaneous velocities obtained by following the displacements of the GPIb-expressing cells as they roll on vWF-A1 surface. Fig. 4, *A–C*, show, respectively, representative velocity profiles in each individual frame of Q232V, WT, and K237V cells rolling on surfaces coated with 100 μg/ml vWF-A1 at a shear stress of 1.6 dyn/cm$^2$. The K237V cells roll more slowly and continuously while the Q232V cells show predominantly saltatory motion punctuated by brief rolling events compared to the WT. To examine the stability of rolling, we determined distribution of rolling durations for many Q232V, WT, and K237V cells. Fig. 4, *D–F*, illustrate the distribution of rolling durations for Q232V, WT, and K237V cells, respectively; the contrast is evident. Whereas the longest time for which the Q232V cells roll continuously on the surface is 0.6 s with >90% of the cells lasting on the surface for less than half a second, a significant fraction of K237V cells stayed for the entire duration monitored (10 s) with >70% of the cells rolling for at least 1 s. The WT cells rolled for a maximum period of 2.2 s with >85% of the cells interacting with the surface for <1 s. The average rolling duration calculated based on these distributions is 5.3-fold more for K237V, and 1.8-fold less for Q232V, than for WT (Fig. 4 *H*). We also calculated the distribution of rolling velocities for the three cell types (Fig. 4 *G*). The K237V cells roll much slower than the WT cells, the mode of the distribution being fivefold lower than that of WT. The Q232V rolling distribution indicates a tendency for Q232V cells to roll faster than WT cells. The mean rolling velocity of K237V is 2.15-fold lower, and that of Q232V is 1.26-fold higher, respectively, than that of WT (Fig. 4 *H*).

## Kinetics of tethering of GPIbα expressing cells on vWF-A1 surface

We measured the tethering frequency, which is proportional to the cellular association rate, by calculating the rate at which CHO cells tethered to vWF-A1-coated surfaces at different coating densities and shear stresses (Ramachandran et al., 1999; Dwir et al., 2000; Chateau et al., 2001). The

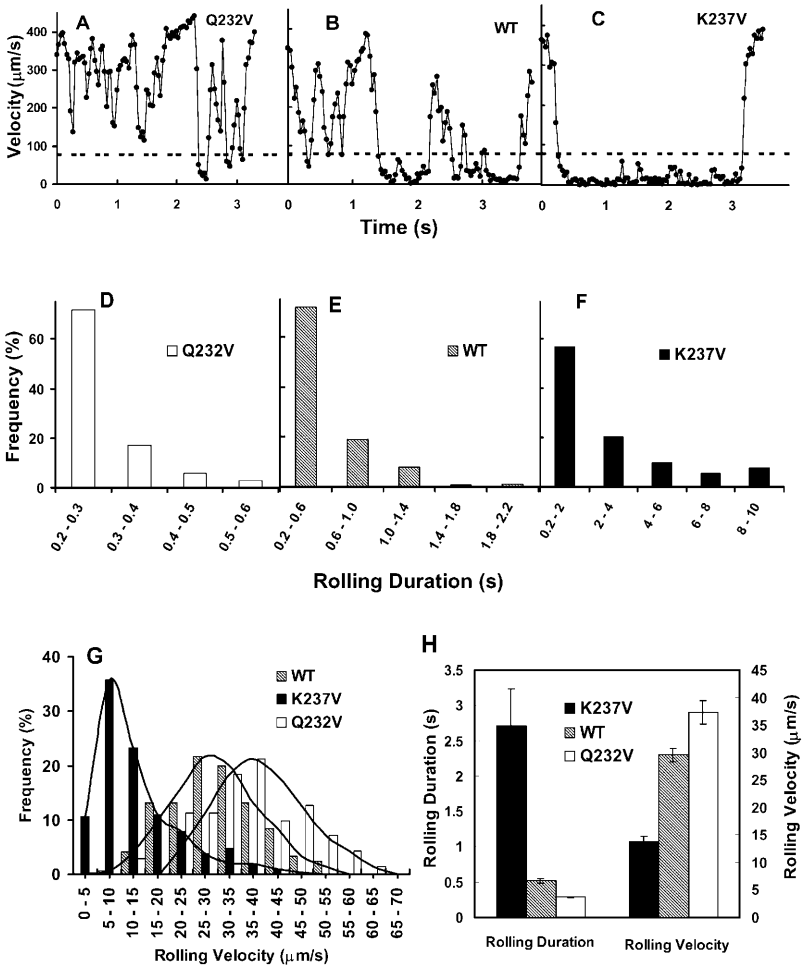


FIGURE 4 Kinetics of rolling of cells expressing wild-type or mutant GPIb receptors at 1.6 dyn/cm$^2$ shear stress on surfaces coated with 100 $\mu$g/ml vWF-A1: Only cells that stayed in contact with the surface for at least 0.2 s were considered for rolling analysis. (*A*, *B*, and *C*) represent the instantaneous velocity profiles of Q232V, WT, and K237V cells. The dashed line denotes the velocity threshold value of 80 $\mu$m/s used to separate the cells free in flow from those that contact and roll on the surface (see Materials and Methods). (*D*, *E*, and *F*) Distribution of rolling duration for the Q232V, WT, and K237V cells. (*G*) Distribution of rolling velocities for the Q232V, WT, and K237V cells. (*H*) Average rolling duration and average rolling velocity while in contact with the surface. The values are based on at least 150 cells for WT and K237V and 60 cells for Q232V, each followed for a maximum of 10 s, averaged from three to five independent experiments.

initial tethering frequency on surfaces coated with 100 $\mu$g/ml vWF-A1 solution at different shear stresses is shown in Fig. 5 *A*. In general, the tethering frequency decreases with an increase in shear stress, possibly due to the decreased time of contact. At any given shear stress, more K237V cells tethered than Q232V or WT cells. The tethering frequency of K237V was threefold greater than WT, which was again threefold greater than Q232V, implying that the rate of bond formation ($k_{on}$) for the gain-of-function mutant is nearly 10-fold more than that of the loss-of-function mutant. We also determined the effect of vWF-A1 coating concentration on the tethering rate. Fig. 5 *B* shows the results at a shear stress of 1.2 dyn/cm$^2$ and it can be seen that at low vWF-A1 coating concentration (10 $\mu$g/ml), although hardly any Q232V and WT cells interact with the vWF-A1-coated surfaces, a significant number of K237V cells tether to the surface. An increase in vWF-A1 coating concentration to 100 $\mu$g/ml increases the tethering frequency of all the cell types.

Moreover, the examination of the videotapes indicated that the two mutants differed not just in the rate of capture from the flowing stream, but also in the ability to sustain interactions with the surface. The Q232V mutant detached after traveling very short distances for a short period of time while K237V stayed on the surface for longer durations traveling longer distances. This prompted us to analyze the fate of the cells once they have tethered to the surface by examining the distance traveled on the vWF-A1 surface before joining the fluid stream. The measured distances were grouped in bins of 5 $\mu$m and the number of cells in each group was expressed as a percent of the total number of cells tethered. A typical plot at a shear stress of 1.6 dyn/cm$^2$ on 100 $\mu$g/ml vWF-A1 is shown in Fig. 5 *C*. The Q232V mutants travel predominantly short distances (>95% travel less than one-half the cell diameter) and the K237V mutants travel predominantly long distances (>70% travel at least one cell diameter) whereas the WT move distances intermediate between those of the two mutants.

Although the short travel distances likely represent the stretching of the tethers or extension of cell membrane, longer travel distance are due to the breakage of old bonds in the rear edge and formation of new ones in the front. Hence we classified tethers that last <5 $\mu$m distance as transient tethers and those of >5 $\mu$m distance as rolling tethers. Fig. 5 *D* shows the percentage of transient and rolling tethers at

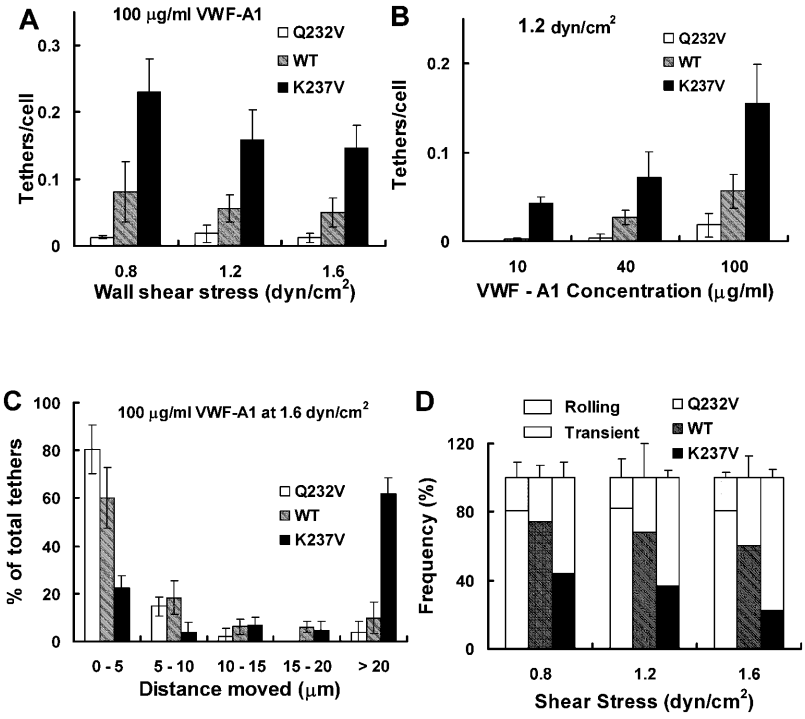


FIGURE 5 Kinetics of tethering of CHO cells expressing WT or mutant GPIb to vWF-A1 surfaces: Initial rate of tethering of CHO cells expressing WT or Q232V or K237V mutants (*A*) to surfaces coated with 100 $\mu$g/ml vWF-A1 at the indicated shear stresses and (*B*) at a shear stress of 1.2 dyn/cm$^2$ on surfaces coated with different concentrations of vWF-A1. (*C*) The distance traveled by tethered cells at 1.6 dyn/cm$^2$ shear stress before detachment from surfaces coated with 100 $\mu$g/ml vWF-A1. The cell diameter is ~15 $\mu$m. (*D*) The fraction of the cells that are transiently tethered before detachment or converted to rolling adhesion. The data presented are means ± SD of three to five experiments.

0.8, 1.2, and 1.6 dyn/cm$^2$ on surfaces coated with 100 $\mu$g/ml vWF-A1. Again, we observe that the K237V cells have much greater efficiency in converting transient tethers to rolling tethers than the WT or the Q232V cells. The fraction of cells that form rolling tethers increases with increase in shear stress for WT and K237V but is unaffected for Q232V.

## Kinetics of dissociation and mechanical strength of GPIbα-vWF-A1 transient tethers

The alteration in the affinities between the wild-type, gain-of-function, and loss-of-function mutants represent differences in the association or dissociation rates of the GPIbα-vWF-A1 bonds. The tethering rate, which reflects cellular $k_{on}$, seems to be significantly affected by the mutations. We also studied the effect of mutations on the tether dissociation rate ($k_{off}$) and hence we measured the lifetime of transient tether durations, which may represent single adhesive bonds (Alon et al., 1997; Smith et al., 1999; Ramachandran et al., 1999). At vWF-A1 coating densities that would not support continuous rolling, the interaction of the cells with the surface was characterized by discrete ratchetlike steps that can be quantified using the time-distance trajectories. The time spent by the cell on the surface with little or no movement (<3 $\mu$m) is defined as pause duration. Fig. 6 *A* shows a representative semilog plot of pause-time distribution at different shear stresses for WT. The tether lifetime appears to obey first-order kinetics and the slope of the line $= -k_{off}$. The $k_{off}$ values increase with an increase in shear stress indicating that the tether lifetime decreases as the force on the bonds increases. Fig. 6 *B* is a similar plot at 0.8 dyn/cm$^2$ and it can be seen that the $k_{off}$ values of Q232V and WT are 2- and 1.5-fold greater, respectively, than that of K237V. The good linear fit may suggest, though not prove, the measurement of a single bond or a quantal unit that mediates the interaction. We do not know the exact number of molecular bonds involved in the tether structure. Nevertheless, these $k_{off}$ values represent the lifetimes of the smallest functional unit of adhesion that permits the cell interaction with the surface and is a useful estimate of the intrinsic kinetic and mechanical properties of the receptor-ligand pairs.

To relate the effect of fluid force on the $k_{off}$, we used the Bell model (1978): $k_{off} = k^0_{off} \exp(\sigma F_b/kT)$ to fit the $k_{off}$ values measured at different shear stresses. In this equation, $F_b$ is the force on the tether bond, $k$ is the Boltzmann constant and $T$ is absolute temperature. The Bell model parameters $k^0_{off}$ and $\sigma$ are the zero-force dissociation constant and reactive compliance, respectively. The higher the $k^0_{off}$ value, the lower the bond lifetime, and the higher the $\sigma$ value, the greater the sensitivity to force-induced dissociation. The net force acting on the tether, $F_b$, because of fluid shear force and torque can be related to the wall shear using the lubrication theory of Goldman et al. (1967) (Fig. 6 *C*). We have fit the $k_{off}$ values measured at various shear stresses to the Bell model (1978) in terms of $F_b$. and the plot is shown in Fig. 6 *D* (Chateau et al., 2001; Ramachandran et al., 2001). It can be seen that the tether bonds of both the mutants and the wild-type are more prone to dissociation with an increase in force. We estimated the $k^0_{off}$ values (in s$^{-1}$) for WT, K237V, and Q232V to be 5.66 ± 0.55, 2.56 ± 0.62, and 7.15 ± 1.18, and the corresponding $\sigma$ values (in Å) to be 0.058 ± 0.007, 0.089

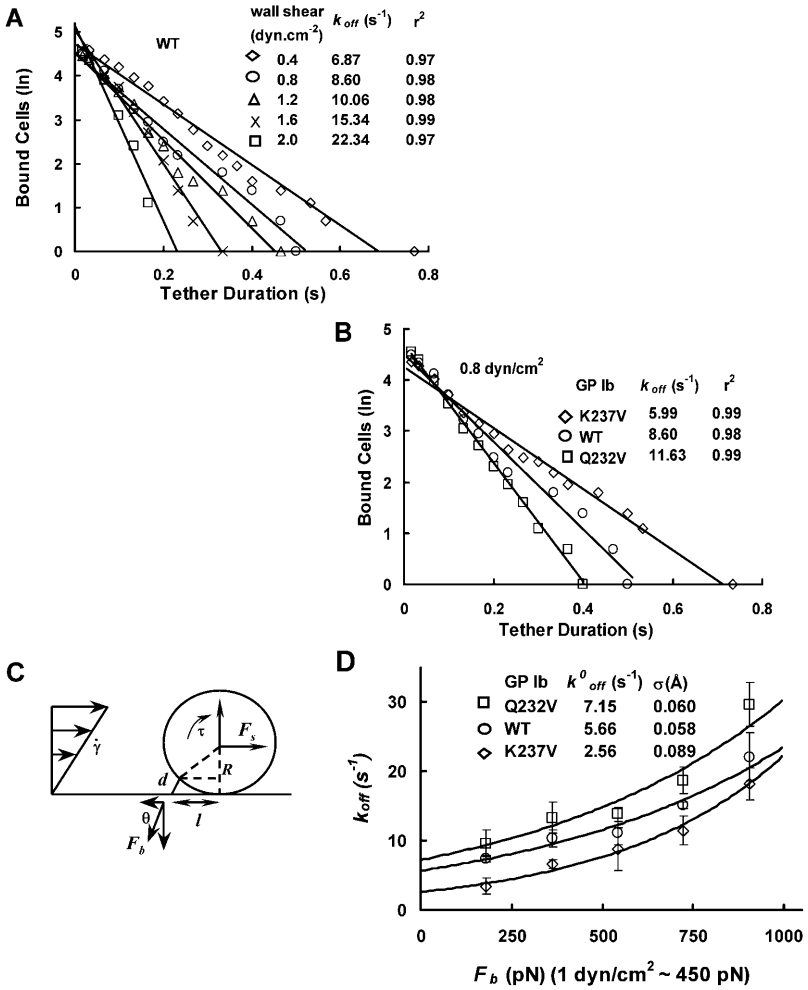


FIGURE 6 Kinetics of dissociation of transiently tethered CHO cells expressing WT or mutant GPIb on vWF-A1 coated surfaces. (*A*) The natural logarithm of the number of cells that remain tethered is plotted as a function of time after initiation of the tether. The negative of the slope is $k_{off}$. The $k_{off}$ decreases with an increase in shear stress for WT (*B*) A plot of first-order dissociation kinetics for WT, Q232V, and K237V at 0.8 dyn/cm$^2$. The $k_{off}$ of Q232V is twice as much as that of K237V. (*C*) Estimation of force on the GPIb$\alpha$-vWF-A1 tether bond. The Goldman equation was used to calculate the hydrodynamic torque, $\tau$, and force, $F_s$, on the cell. The force and torque balances on a tethered cell in shear flow are $F_s = F_b \cos\theta$ and $F_b l \sin\theta = \tau_s + R F_s$, where $R$ is the cell radius and $l$ is the lever arm. Calculation with $R = 8.5$ $\mu$m and $\theta = 60^\circ$ yielded the force on the tether bond, $F_b$ ~450 pN/(dyn/cm$^2$). (*D*) We used the Bell model (see text) to fit the experimental data. At each shear stress, 150–250 events were collected and each point represents the mean from three different experiments. Error bars show SD. The data were fit to the Bell equation, $k_{off} = k^0_{off} \exp(\sigma F_b/kT)$.

$\pm$ 0.013, and 0.06 $\pm$ 0.01, respectively. It can be seen that the $k^0_{off}$ value of WT is 1.25-fold lower, and 2.2-fold greater, than Q232V and K237V, respectively. The $\sigma$ value of Q232V is comparable to WT but that of K237V is ~1.5-fold greater than the WT.

## DISCUSSION

Quantification of the interactions of platelet GPIb$\alpha$ with vWF-A1 domain can help us better understand the mechanisms that result in altered phenotypes caused by mutations in the receptor or the ligand. We have shown earlier that the gain- and loss-of-function mutants of GPIb$\alpha$ have altered affinities for vWF by modulator titration and in flow chamber assays (Dong et al., 2000, 2001). Here, we characterized these differences by analyzing the basic kinetics of the interaction between vWF-A1 and wild-type GPIb$\alpha$, and gain- and loss-of-function GPIb$\alpha$ mutants under controlled flow conditions. We calculated the cellular association rate constants (tethering frequencies) and dissociation rate constants (tether lifetimes) at different shear stresses and coating densities. Wild-type GPIb$\alpha$ has a 1.25-fold higher and 2.2-fold lower unstressed dissociation rate constant than the loss- and gain-of-function mutants, respectively. On the other hand, the tethering frequency of WT GPIb$\alpha$ is threefold higher and threefold lower than that of loss- and gain-of-function mutants, respectively. These changes in both the on- and off-rates likely account for the phenotypic manifestations of these mutations.

We made several observations that highlight the remarkable changes in the GPIb-vWF-A1 interaction caused by the GPIb$\alpha$ mutations K237V and Q232V. First, very few K237V cells could be seen to roll continuously at vWF-A1 coating concentrations as low as 5 $\mu$g/ml, whereas many of the Q232V cells did not roll continuously even at a vWF-A1 concentration as high as 150 $\mu$g/ml. The WT showed predominantly saltatory motion in this concentration range (data not shown). Second, the K237V cells converted transient tethers to rolling tethers (at 1.6 dyn/cm$^2$ on surfaces coated with 100 $\mu$g/ml vWF-A1) much more efficiently (50–75%) than Q232V cells (10–20%) and WT cells (25–40%) (Fig. 5 *D*). Third, the average rolling velocity of Q232V cells was 1.26-fold faster and that of K237V cells 2.15-fold slower than that of the WT (Fig. 4). Fourth, the average

rolling duration (the time spent by a rolling cell in continuous contact with the surface), was approximately twofold less for Q232V and approximately fivefold more for K237V cells compared to the WT.

Rolling adhesion is an inherently unstable transition state, delicately poised between firm adhesion and lack of adhesion. Maintenance of stable rolling requires that the average number of bonds that are formed and broken be nearly equal. The rate of bond formation is related to the cellular association rate constant, $k_{on}$, and the rate of bond dissociation is quantified by the dissociation rate constant, $k_{off}$. We calculated the $k_{off}$ values for the wild-type and mutant GPIbα interactions with vWF-A1 from measures of the lifetime of transient tethering events. We used low vWF-A1 coating densities that would support tethering but not continuous rolling of the CHO cells so as to minimize the number of bonds that mediate the transient tethering events. By doing so, we have measured the lifetime of the smallest functional unit of the interaction that could be observed at the spatial and temporal resolution employed in this study. The tether time distribution followed first-order dissociation kinetics and has properties that suggest the smallest functional units of interaction behave as single bonds. Although such properties do not prove the absence of multiple bonds, these events are of physiological relevance as they represent the smallest functional unit of adhesion that permits cell interactions in flow. From Table 2, it can be seen that the $k^0_{off}$ values are affected to different degrees by Q232V and K237V mutations. While the K237V mutation results in a 2.2-fold decrease in $k^0_{off}$, the Q232V mutation results in a 1.25-fold increase.

The lifetime ($1/k^0_{off}$) of the GPIbα-vWF-A1 bond we have measured compares very well with the lifetime of selectin-carbohydrate bonds (Table 2) measured using various techniques including flow chamber assays and surface plasmon resonance (Alon et al., 1997; Mehta et al., 1998; Ramachandran et al., 1999). The selectin-carbohydrate bond performs the function of recruiting leukocytes from the flowing bloodstream to the site of inflammation in much the same way that the GPIbα-vWF-A1 bond recruits platelets from flowing blood in hemostasis and thrombosis. Hence, one would expect the kinetic properties of the two classes of bonds to be similar (Konstantopoulos et al., 1998; Doggett et al., 2002, 2003). Our results (Table 2) indicate that this is indeed the case. These bond lifetimes are shorter than those of integrins estimated to be >20 s, which mediate firm adhesion of neutrophils to endothelium (Chateau et al., 2001). The short tether lifetimes of transient interactions like selectin and GPIb bonds are crucial for promoting rolling adhesions (Chang et al., 2000).

Interestingly, the zero-force dissociation constant ($k^0_{off}$) value for the GPIbα-vWF-A1 interaction obtained by us is significantly higher (~1500-fold) than that reported by Miura et al. (2000). This discrepancy could be due to the use of solution-phase biochemical assay as opposed to our measurements under dynamic flow conditions. The static assay is likely to underestimate the impact the mechanical forces on the bond lifetime. This possibility is supported by the recent work of Doggett et al. (2002). They reported the dissociation rate constant of GPIbα on immobilized platelets and vWF-A1-coated beads using a flow chamber assay to be 3.21 $s^{-1}$, a value close to that obtained in this work (Table 2). It should be noted that the force on the GPIb tether bond on the CHO cell surface at a shear stress of 1 dyn/$cm^2$ used in our experiments compares roughly to that of 20 dyn/$cm^2$ experienced by the platelet tether bond, given the 5- to10-fold size difference between platelets and CHO cells (Fredrickson et al., 1998).

In addition to $k^0_{off}$, we also measured the tethering frequency, the rate at which cells tether to the vWF-A1 surface from free flow. The tethering frequency is proportional to the rate of formation of the initial bond, provided the bond is sufficiently strong and long-lived to be observed and if the fraction of cells that is tethered to the surface for durations shorter than the sampling rate is small. The tethering frequency can be viewed as a lumped cellular association rate constant ($k_{on}$), being dependent on hydrodynamic parameters like shear rate and relative velocity of the approaching surfaces, physical parameters like the distribution and orientation of receptor and ligand moieties as well as the intrinsic association rate constant. At a given shear stress (assuming comparable receptor and ligand

**TABLE 2 Kinetic and mechanical properties of receptor-ligand tether bonds**

| Receptor | Ligand | $k^0_{off}$ ($s^{-1}$) | σ (Å) | Reference |
|---|---|---|---|---|
| GPIbα (WT) | vWF-A1(WT) | 5.66 | 0.058 | This work |
| GPIbα (Q232V) | vWF-A1(WT) | 7.15 | 0.06 | This work |
| GPIbα (K237V) | vWF-A1(WT) | 2.56 | 0.089 | This work |
| GPIbα (WT) | vWF-A1(WT) | 0.0038 | — | Miura et al. (2000) |
| GPIbα (WT) | vWFA1(type2B) | 0.0036 | — | Miura et al. (2000) |
| GPIbα (WT) | vWF-A1(WT) | 3.21 | 0.18 | Doggett et al. (2002) |
| GPIbα (WT) | vWF-A1(type2B) | 0.56 | 0.26 | Doggett et al. (2002) |
| GPIbα (G233V) | vWF-A1(WT) | 0.55 | 0.29 | Doggett et al. (2003) |
| L-selectin | PNAd | 6.80 | 0.2 | Alon et al. (1997) |
| P-selectin | PSGL-1 | 1.1 | 0.29 | Ramachandran et al. (1999) |
| α4β7/Ca | MAdCAM-1 | 0.046 | 0.91 | Chateau et al. (2001) |

densities), the differences in the tethering frequency will be a surrogate measure of the intrinsic differences in the $k_{on}$ due to mutations (Ramachandran et al., 1999; Dwir et al., 2000; Chateau et al., 2001). In general, the tethering frequency decreases with increasing shear stress (Fig. 5 *A*) due to shorter contact time between the reacting surfaces. At any given shear stress, the tethering frequency of WT was higher than Q232V and lower than K237V. In fact, the mutations resulted in a threefold lower tethering rate for Q232V and a threefold increase for K237V. Also, the tethering frequency of K237V at vWF-A1 coating concentrations as low as 10 $\mu$g/ml is more than that of Q232V at a concentration as high as 100 $\mu$g/ml (Fig. 5 *B*).

Cell rolling depends on the efficiency of converting transient tethers to stable tethers by forming new tether bonds in the front edge as the old tether bonds in the rear edge dissociate. We have shown that the gain-of-function mutation leads to an increase in the cellular association rate (quantified by tethering frequency) of threefold and a decrease in dissociation rate (quantified by tether lifetime) of 2.2-fold. In contrast, the loss-of-function mutation results in a threefold decrease in the cellular association rate and a 1.25-fold increase in the dissociation rate. The composite effect of these kinetic changes for K237V is manifested by an approximately fivefold increase in the rolling duration and by an approximately twofold decrease for Q232V. The close agreement in fold differences in the rolling velocities and off-rate constants—1.26-fold increase for Q232V and 2.15-fold decrease for K237V compared to WT in rolling velocity —indicate that the rolling velocities are dependent more on the rate at which bonds break than the rate at which bonds form.

The clinical implications of changes in off- and on-rate due to the K237V mutation can be extrapolated to the naturally occurring G233V mutations associated with ptVWD. An increase in the rate of formation of GPIb$\alpha$-vWF-A1 bond results in an increase in the rate of fruitful ptVWD platelet-vWF encounters and the prolongation in the lifetime of the existing bonds greatly enhances the probability of spontaneous aggregation of ptVWD platelets compared to normal platelets. The characteristics of this ligand-receptor bond that has evolved in humans thus represents a tight balance between allowing adequate platelet tethering at the site of vessel injury and preventing the spontaneous binding and clearance of hemostatically active vWF multimers present in the circulating blood.

Other investigators have attributed the increase in affinity associated with the gain-of-function mutations of either GPIb$\alpha$ or vWF-A1 to both increases in the association rate and decreases in the dissociation rate. Miura et al. (2000) reported a fourfold increase in $k_{on}$ as the *sole* reason for increased affinity of G233V GPIb$\alpha$ mutant over wild-type while Doggett et al. (2002) reported a fivefold decrease *only* in $k_{off}^0$ as a reason for increased affinity for the I546V gain-of-function mutant of vWF-A1. The discrepancy between our work and that of Miura et al. (2000) could be attributed to the differences between the static and dynamic adhesion assays used. Although Doggett et al. (2002) also used a dynamic flow adhesion assay, they did not determine the role of on-rate in observed mutant and wild-type phenotype. Very recently, Doggett et al. (2003) reported the alteration in the kinetics of GPIb-vWF-A1 bond associated with the G233V mutation in GPIb$\alpha$. By perfusing vWF-A1-coated beads over a surface of immobilized platelets, they observed an enhancement in the tethering rate and also a decrease in the dissociation rate constant of the GPIb$\alpha$-vWF-A1 tether bond in the gain-of-function mutant. As shown in Table 2, the $k_{off}^0$ value estimated in their study compares very well with this work. The discrepancy in the reactive compliance $\sigma$ between the present study and that of Doggett et al. (2003), could be attributed to several possibilities including: 1), differences in the number, orientation, and distribution of receptors and ligands on the immobilized platelet-bead system of Doggett et al. (2003) versus immobilized ligand-free-flowing cell system used in the present study; 2), differences in the size and mechanical properties of cells versus those of the beads and hence the force experienced by the tether bond; 3), possible extension of tethers from immobilized platelet surface or from the cell surface, which can alter the estimates on the force experienced by the tether bond; or 4) though very unlikely, under-sampling of short-lived events at 30 fps resulting in the underestimation of off-rate constant at the highest shear stress, in the present work.

Our results also indicate that mutations altering the GPIb$\alpha$- vWF-A1 kinetics could be fundamentally different from some of the mutations altering selectin bond kinetics, despite the many similarities. Single tyrosine mutations in PSGL-1 have been shown to affect the affinity of neutrophil P- and L- selectins as manifested by differences in rolling behavior. These differences were due primarily to the alterations in dissociation rate as association rate remains unaffected (Ramachandran et al., 1999). Further, of the two components that determine the measured dissociation rate—the reactive compliance, $\sigma$, and the zero-force dissociation rate constant, $k_{off}^0$—these authors found that PSGL-1 mutations alter P-selectin-PSGL-1 interaction by altering the $\sigma$ but $k_{off}^0$ is unaffected whereas the same mutation alters the L-selectin-PSGL-1 interaction by altering the $k_{off}^0$ without affecting $\sigma$. In contrast, our findings with the GPIb$\alpha$-vWF-A1 bond indicate that the $\sigma$ value is unchanged by the Q232V mutation but increases by 1.5-fold for the K237V mutation (Table 2). Since the $\sigma$ value represents the mechanical flexibility of the bond, it is probable that the moderate increase in the reactive compliance of the K237V GPIb$\alpha$-vWF-A1 bonds may compensate for an already low $k_{off}^0$.

In summary, we have characterized the kinetics of a physiologically and medically very important interaction between platelet glycoprotein Ib$\alpha$ and vWF-A1. Our findings show that these bonds have a rapid dissociation

kinetics, similar to selectin bonds, ideally suited for surveillance by platelet rolling on immobilized vWF at sites of vessel wall injury before adhering firmly to form thrombi. Comparison of the association and dissociation rates of gain- and loss-of-function mutations with wild-type showed an alteration in both of these quantities which might provide some mechanistic explanation to the observed differences in rolling behavior and affinities for these mutants with plasma vWF. Our results shed some light on understanding and possibly treating clinical abnormalities like ptVWD disease, which has a functional phenotype similar to the K237V mutant.

R.A.K. thanks Drs. Shih-Hsin Kao and Vishy Ramachandran for helpful discussions and Jody Whitelock for technical assistance.

This work was supported by National Institutes of Health grants HL-18672 and HL-65967, the Robert A. Welch Foundation grant C-938, and a grant from the Mary R. Gibson Foundation.

## REFERENCES

Alon, R., S. Chen, K. D. Puri, E. B. Finger, and T. A. Springer. 1997. The kinetics of L-selectin tethers and the mechanics of selectin-mediated rolling. *J. Cell Biol.* 138:1169–1180.

Andrews, R. K., J. A. Lopez, and M. C. Berndt. 1997. Molecular mechanisms of platelet adhesion and activation. *Int. J. Biochem. Cell Biol.* 29:91–105.

Bell, G. I. 1978. Models for the specific adhesion of cells to cells: a theoretical framework for adhesion mediated by reversible bonds between cell surface molecules. *Science.* 200:618–627.

Berndt, M. C., Y. Shen, S. M. Dopheide, E. E. Gardiner, and R. K. Andrews. 2001. The vascular biology of the glycoprotein Ib-IX-V complex. *Thromb. Haemost.* 86:178–188.

Chang, K. C., D. F. J. Tees, and D. A. Hammer. 2000. The state diagram for cell adhesion under flow: leukocyte rolling and firm adhesion. *Proc. Natl. Acad. Sci. USA.* 144:185–200.

Chateau, M., S. Chen, A. Salas, and T. A. Springer. 2001. Kinetic and mechanical basis of rolling through an integrin and novel $Ca^{2+}$-dependent rolling and $Mg^{2+}$-dependent firm adhesion modalities for the $\alpha 4\beta 7$-MAdCAM-1 interaction. *Biochemistry.* 40:13972–13979.

Cruz, M. A., T. G. Diacovo, J. Emsley, R. Liddington, and R. I. Handin. 2000. Mapping the glycoprotein Ib-binding site in the von Willebrand factor A1 domain. *J. Biol. Chem.* 275:19098–19105.

Doggett, T. A., G. Giridhar, A. Lawshe, D. W. Schmidtke, I. J. Laurenzi, S. L. Diamond, and T. G. Diacovo. 2002. Selectin-like kinetics and biomechanics promote rapid platelet adhesion in flow: the GPIb$\alpha$-vWF tether bond. *Biophys. J.* 83:194–205.

Doggett, T. A., G. Giridhar, A. Lawshe, J. L. Miller, I. J. Laurenzi, S. L. Diamond, and T. G. Diacovo. 2003. Alterations in the intrinsic properties of the GPIb$\alpha$-VWF tether bond define the kinetics of the platelet-type von Willebrand disease mutation. *Blood.* 102:152–160.

Dong, J., M. C. Berndt, A. Schade, L. V. McIntire, R. K. Andrews, and J. A. Lopez. 2001. Ristocetin-dependent, but not botrocetin-dependent binding of von Willebrand factor to the platelet glycoprotein Ib-IX-V complex correlates with shear-dependent interactions. *Blood.* 97:162–168.

Dong, J., A. J. Schade, G. M. Romo, R. K. Andrews, S. Gao, L. V. McIntire, and J. A. Lopez. 2000. Novel gain-of-function mutations of platelet glycoprotein Ib $\alpha$ by valine mutagenesis in the Cys209-Cys248 disulfide loop. *J. Biol. Chem.* 275:27663–27670.

Dwir, O., G. S. Kansas, and R. Alon. 2000. An activated L-selectin mutant with conserved equilibrium binding properties but enhanced ligand recognition under shear flow. *J. Biol. Chem.* 275:18682–18691.

Fredrickson, B. J., J. Dong, L. V. McIntire, and J. A. López. 1998. Shear-dependent rolling on von Willebrand factor of mammalian cells expressing the platelet glycoprotein Ib-IX-V complex. *Blood.* 92: 3684–3693.

Goldman, A. J., R. G. Cox, and H. Brenner. 1967. Slow viscous motion of a sphere parallel to a plane wall. II. Couette flow. *Chem. Eng. Sci.* 22:653–660.

Huizinga, E. G., S. Tsuji, R. A. P. Romijn, M. E. Schiphorst, P. G. de Groot, J. J. Sixma, and P. Gros. 2002. Structures of glycoprotein Ib $\alpha$ and its complex with von Willebrand factor A1 domain. *Science.* 297: 1176–1179.

Konstantopoulos, K., S. Kukreti, and L. V. McIntire. 1998. Biomechanics of cell interactions in shear fields. *Adv. Drug Deliv. Rev.* 33:141–164.

López, J. A. 1994. The platelet glycoprotein Ib-IX complex. *Blood Coagul. Fibrinolysis.* 5:97–119.

López, J. A., B. Leung, C. C. Reynolds, T. Sih, M. Chambers, and C. Q. Li. 1994. Glycoprotein (GP) Ib $\beta$ is the critical subunit linking GPIb$\alpha$ and GP IX in the GPIb-IX complex: analysis of partial complexes. *J. Biol. Chem.* 269:23716–23721.

López, J. A., and J. Dong. 1997. Structure and function of the glycoprotein Ib-IX-V complex. *Curr. Opin. Hematol.* 4:323–329.

Mehta, P., R. D. Cummings, and R. P. McEver. 1998. Affinity and kinetic analysis of P-selectin binding to P-selectin glycoprotein ligand-1. *J. Biol. Chem.* 273:32506–32513.

Miller, J. L. 1996. Platelet-type von Willebrand disease. *Thromb. Haemost.* 75:865–869.

Miura, S., C. Q. Li, Z. Cao, H. Wang, M. R. Wardell, and J. E. Sadler. 2000. Interaction of von Willebrand factor domain A with platelet glycoprotein Ib $\alpha$-(1–289). *J. Biol. Chem.* 275:7539–7546.

Miyata, S., and Z. M. Ruggeri. 1999. Distinct structural attributes regulating von Willebrand factor A1 domain interaction with platelet glycoprotein Ib $\alpha$ under flow. *J. Biol. Chem.* 274:6586–6593.

Ramachandran, V., M. U. Nollert, H. Qiu, W.-J. Liu, R. D. Cummings, C. Zhu, and R. P. McEver. 1999. Tyrosine replacement in P-selectin glycoprotein ligand-1 affects distinct kinetic and mechanical properties of bonds with P- and L-selectin. *Proc. Natl. Acad. Sci. USA.* 96: 13771–13776.

Ramachandran, V., T. Yago, T. K. Epperson, M. M. A. Kobzdej, M. U. Nollert, R. D. Cummings, C. Zhu, and R. P. McEver. 2001. Dimerization of a selectin and its ligand stabilizes cell rolling and enhances tether strength in shear flow. *Proc. Natl. Acad. Sci. USA.* 98:10166–10171.

Ross, J. M., B. R. Alevriadou, and L. V. McIntire. 1998. Rheology. *In* Thrombosis and Hemorrhage. J. Loscalzo and A. I. Schafer, editors. Williams & Wilkins, Wroclaw, Poland. 405–421.

Shen, Y., G. M. Romo, J. Dong, A. Schade, L. V. McIntire, D. Kenny, J. C. Whisstock, M. C. Berndt, J. A. López, and R. K. Andrews. 2000. Requirement of leucine-rich repeats of glycoprotein (GP) Ib $\alpha$ for shear-dependent and static binding of von Willebrand factor to the platelet membrane GPIb-IX-V complex. *Blood.* 95:903–910.

Sadler, J. E. 1998. Biochemistry and genetics of von Willebrand factor. *Annu. Rev. Biochem.* 67:395–424.

Slack, S. M., and V. T. Turitto. 1994. Flow chambers and their standardization for use in studies of thrombosis. On behalf of the subcommittee on Rheology of the Scientific and Standardization Committee of the ISTH. *Thromb. Haemost.* 72:777–781.

Smith, M. J., E. L. Berg, and M. B. Lawrence. 1999. A direct comparison of selectin-mediated transient, adhesive events using high temporal resolution. *Biophys. J.* 77:3371–3383.